Bond Strengths in $ChCl_3^-$ and $ChOCl_3^-$ (Ch = S, Se, Te): Experiment and Theory

Kim C. Lobring,† Changtong Hao,† Jordan K. Forbes,‡ Michael R. J. Ivanov,† Steven M. Bachrach,*,‡ and Lee S. Sunderlin*,†

Department of Chemistry and Biochemistry, Northern Illinois University, DeKalb, Illinois 60115, and Department of Chemistry, Trinity University, 1 Trinity Place, San Antonio, Texas 78212

Received: March 31, 2003

The strengths of the $SeCl_2-Cl^-$, $SeOCl_2-Cl^-$, $SeBr_2-Br^-$, and $TeCl_2-Cl^-$ bonds have been measured to be 133 ± 9, 150 ± 10, 110 ± 6, and 170 ± 7 kJ mol^{-1}, respectively, by determining thresholds for collision-induced dissociation in a flowing afterglow-tandem mass spectrometer. These values are stronger than the previously measured $D(SCl_2-Cl^-)$ and $D(SOCl_2-Cl^-)$, both 85 ± 8 kJ mol^{-1}. Bond energies and other properties for these molecules and $TeOCl_3^-$ have also been computed by several high-level computational techniques, including B3LYP/aug-cc-pVTZ. There is excellent agreement between the experimental and computational energetics for $SeCl_3^-$, $SeOCl_3^-$, and $TeCl_3^-$. The bond strengths increase in the order S < Se < Te.

Introduction

We have recently performed experimental measurements and computational studies of the bond strengths in the hypervalent anions SCl_3^- and $SOCl_3^-$.[1,2] These anions are termed hypervalent[3−10] (or hypercoordinate) because their electron dot structures show 10 electrons around the sulfur atom. Although these anions violate the octet rule, the bonds are reasonably strong: $D(SCl_2-Cl^-)$ and $D(SOCl_2-Cl^-)$ are both 85 ± 8 kJ mol^{-1}.[1,2]

Extension of this work to the other chalcogenides, selenium and tellurium, is interesting for several reasons. One is the exploration of periodic trends in bond strengths. Bond strengths in hypervalent systems are strongly correlated with several properties of the atoms involved in the bonding, such as electronegativity.[11] Sulfur and selenium have very similar Pauling electronegativities, while that for Te is lower (2.58, 2.55, and 2.1, respectively). Other electronegativity scales give similar results.[12] A comparison of these trichlorides gives additional data regarding which atomic properties are best correlated with bond strength.

Comparing $ChCl_3^-$ and $ChOCl_3^-$ (Ch = chalcogenide: S, Se, or Te) also gives further insight into the effect of oxidation on hypervalent bond strengths. There has been some previous work on related molecules. Larson and McMahon[13] determined that the bond energy in POF_4^- was 32 kJ mol^{-1} higher than the bond energy in PF_4^-. In contrast, the bond energy in $POCl_4^-$ is 47 kJ mol^{-1} weaker than in PCl_4^-; this difference is attributable to the high energy cost of the rearrangement necessary to prepare $POCl_3$ for bonding an additional chloride.[14] Thus, the effect of an oxygen ligand on bond strengths in these ions is not easily predicted. Unfortunately, it was not possible to make a sufficient flux of $TeOCl_3^-$ for CID experiments, but computational results are given below.

Although it would be useful to compare the chalcogenide chlorides to the corresponding bromides, some of these experiments are not feasible because of limitations on precursors or instrumentation. SBr_2 is not stable at room temperature,[15] ruling out experiments on SBr_3^-. The boiling point of $TeBr_4$ is too high (414 °C)[15] to allow a sufficient quantity of $TeBr_3^-$ to be made. However, experiments on $SeBr_3^-$ were performed and are discussed below.

We have also been interested in the mechanism of nucleophilic substitution at heteroatoms, especially at sulfur and selenium. For gas-phase substitution of sulfur in sulfides,[16] disulfides,[17] and trisulfides,[18] the mechanism is addition−elimination. The S_N2 mechanism operates only when strain precludes the formation of the hypercoordinate intermediate,[19] such as for the reaction of dithiirane or 1,2-dithietane with HS^-. The addition−elimination mechanism also holds for nucleophilic substitution at selenium in simple diselenides and selenosulfides.[20] Our earlier studies[1,2] of SCl_3^- and $SOCl_3^-$ were motivated by the desire to dramatically stabilize the hypercoordinate intermediate on the addition−elimination pathway. The same motivation applies here: can placement of electron-withdrawing groups on selenium or tellurium lead to a very stable hypercoordinate intermediate?

Some information is known about the ions involved in this study. The stability of $SeOCl_3^-$ has been measured in dimethyl sulfoxide (DMSO) solution,[21] where the bond enthalpy at 298 K is 24.3 kJ mol^{-1}. LaHaie and Milne[22] measured the infrared and Raman spectra of $(C_2H_5)_4N^+SeOCl_3^-$, and Paetzold and Aurich[23] measured the Raman spectra of $K^+SeOCl_3^-$. A general review of hypervalent organochalcogen chemistry has been published recently.[24] Computational results for the anions are lacking, although Dobado et al.[25] have studied molecules such as $SeOF_2$ using computational techniques similar to those used in this paper, two groups[26,27] have performed calculations on neutral hypervalent S-, Se-, and Te-containing compounds, and Schaefer and co-workers[28] have performed calculations on SeF_n and SeF_n^- ($n = 1-7$).

Experimental Section

Bond strengths were measured by the energy-resolved collision-induced dissociation (CID) technique[29,30] in a flowing

* Corresponding authors: (LSS) sunder@niu.edu; phone 815-753-6870; (SMB) sbachrach@trinity.edu; phone 210-999-7379.
† Northern Illinois University.
‡ Trinity University.

10.1021/jp030388v CCC: $25.00
Published on Web 11/20/2003

afterglow-tandem mass spectrometer (MS).[31] The instrument consists of an ion source region, a flow tube, and the tandem MS. The DC discharge ion source used in these experiments is typically set at 2000 V with 2 mA of emission current. The flow tube is a 92 cm × 7.3 cm i.d. stainless steel pipe that operates at a buffer gas pressure of 0.35 Torr, a flow rate of 200 standard $cm^3\ s^{-1}$, and an ion residence time of 100 ms. The buffer gas is helium with up to 10% argon added to stabilize the DC discharge.

To make $SeOCl_3^-$ for this study, $SeOCl_2$ was added to the ion source. Because of the toxicity and stench of this precursor, the sample was contained in a round-bottomed flask attached to a series of two valves. The $SeOCl_2$ was loaded into the flask in an inert-atmosphere glovebag in a fume hood and was not exposed to the atmosphere thereafter. Electron impact on $SeOCl_2$ produces Cl^-, which adds to an additional $SeOCl_2$ molecule to form $SeOCl_3^-$. On one occasion, Cl_2 was added to the ion source to produce additional Cl^-. Approximately 10^5 collisions with the buffer gas cool the metastable ions to room temperature.

To make $SeCl_3^-$, $SeCl_4$ was admitted to the ion source via a heated sample holder, and an argon flow was directed over the sample to increase the precursor flow into the ion source. Upon evaporation, $SeCl_4$ dissociates to $SeCl_2$ and Cl_2.[15,32] Electron impact on these species gives Cl^-; addition of Cl^- to $SeCl_2$ gives the desired $SeCl_3^-$. Dissociative electron attachment to $SeCl_4$ may also produce $SeCl_3^-$. C_2Cl_4 was added on some occasions to produce more Cl^-. The same method was used to make $TeCl_3^-$ from $TeCl_4$ and $SeBr_3^-$ from $SeBr_4$ except that the argon flow was not directed over the sample for either molecule, and no heat was used for $SeBr_4$.

The tandem MS includes a quadrupole mass filter, an octopole ion guide, a second quadrupole mass filter, and a detector, contained in a stainless steel box that is partitioned into five differentially pumped chambers to ensure that further collisions of the ions with the buffer gas are unlikely after ion extraction. During CID experiments, the ions are extracted from the flow tube and focused into the first quadrupole for mass selection. The reactant ions are then focused into the octopole, which passes through a reaction cell that contains a collision gas (Ar for the lighter reactants, $SeCl_3^-$ and $SeOCl_3^-$, and Xe for the heavier reactants, $SeBr_3^-$ and $TeCl_3^-$). After the dissociated and unreacted ions pass through the reaction cell, the second quadrupole is used for mass analysis. The detector is an electron multiplier operating in pulse-counting mode.

The energy threshold for CID is determined by modeling the cross section for product formation as a function of the reactant ion kinetic energy in the center-of-mass (CM) frame, E_{cm}. The octopole is used as a retarding field analyzer to measure the energy zero of the reactant ion beam. The ion kinetic energy distribution is typically Gaussian with an average full-width at half-maximum of 1.0 eV (1 eV = 96.5 kJ mol^{-1}). The octopole offset voltage measured with respect to the center of the Gaussian fit gives the laboratory kinetic energy, E_{lab}, in electronvolts. Low offset energies are corrected for truncation of the ion beam.[33] To convert to the center-of-mass (CM) frame, the equation $E_{cm} = E_{lab}m(m + M)^{-1}$ is used, where m and M are the masses of the neutral and ionic reactants, respectively. All experiments were performed with both mass filters at low resolution to improve ion collection efficiency and reduce mass discrimination. Average atomic masses were used for all elements.

The total cross section for a reaction, σ_{total}, is calculated using eq 1, where I is the intensity of the reactant ion beam, I_0 is the intensity of the incoming beam ($I_0 = I + \Sigma I_i$), I_i is the intensity of each product ion, n is the number density of the collision gas, and l is the effective collision length, 13 ± 2 cm. Individual product cross sections σ_i are equal to $\sigma_{total}(I_i/\Sigma I_i)$.

$$I = I_o \exp(-\sigma_{total} n l) \tag{1}$$

Threshold energies are derived by fitting the data to a model function given in eq 2, where $\sigma(E)$ is the cross section for formation of the product ion at center-of-mass energy E, E_T is the desired threshold energy, σ_0 is the scaling factor, n is an adjustable parameter, and i denotes rovibrational states having energy E_i and population g_i ($\Sigma g_i = 1$). Doppler broadening and the kinetic energy distribution of the reactant ion are also accounted for in the data analysis, which is done using the CRUNCH program written by Armentrout and co-workers.[33]

$$\sigma(E) = \sigma_0 \sum_i g_i (E + E_i - E_T)^n / E \tag{2}$$

Vibrational and rotational frequencies for use in these calculations were calculated at the B3LYP/aug-cc-pVTZ level, which has been demonstrated to be accurate for similar molecules.[34] These frequencies are given in Table 1. For $SeCl_2$ and $SeOCl_2$, the calculated frequencies are lower than the known experimental values[35] by an average of 4% (with a standard deviation of 5%). This is consistent with the 5% ± 3% underestimate seen for both $SOCl_2$[2] and related phosphorus systems.[14] The two sets of experimental vibrational frequencies[22,23] for $SeOCl_3^-$ do not agree with each other or with the calculated frequencies; spectra for similar molecules have been shown to be difficult to assign.[34] Frequency sets for the other molecules involved in this study are incomplete. Therefore, the calculated values are used without further comparison to the previous experimental results.

Uncertainties in the derived thresholds due to possible inaccuracies in the frequencies were estimated by multiplying the entire sets of frequencies by 0.9 and 1.1. The resulting changes in internal energies were less than 1 kJ mol^{-1}. Therefore, the calculated frequencies were used without scaling. Polarizabilities for neutral molecules were also taken from the computational results; varying the rotational constants or polarizabilities has a negligible effect on the derived bond strengths.

Collisionally activated metastable complexes can have sufficiently long lifetimes that they do not dissociate on the experimental time scale (ca. 50 μs). Such kinetic shifts are accounted for in the CRUNCH program by RRKM lifetime calculations. The relatively small molecules studied in this work have small kinetic shifts, less than 1 kJ mol^{-1}. The uncertainty in the derived thresholds is again estimated by multiplying reactant or product frequency sets by 0.9 and 1.1 and by multiplying the time window for dissociation by 10 and 0.1. The effect of these variations is negligible.

An ion not sufficiently energized by one collision with the target gas may gain enough energy in a second collision to be above the dissociation threshold. This effect is eliminated by linear extrapolation of the data taken at several pressures to a zero-pressure cross section before fitting the data.[36]

The reagents $SeCl_4$ and $SeBr_4$ were obtained from Aldrich, $SeOCl_2$ and $TeCl_4$ were obtained from Acros, He and Ar were obtained from BOC, and Xe was obtained from Spectra Gases. All reagents were used as received.

Computational work on these systems was performed with the Gaussian 98 suite.[37] The natural bond orbitals analysis (NBO)[38] program was also used to study the bonding and the

TABLE 1: Vibrational Frequencies and Rotational Constants

compd	exp vib[a] (cm^{-1})	calc vib[b] (cm^{-1})	calc rot.[b] (cm^{-1})	polarizability[b] (10^{-24} cm^3)
$SeCl_3^-$		70.7	0.0288	
		126.9	0.0398	
		128.2	0.1046	
		216.9		
		233.7		
		362.1		
$SeCl_2$	153	154.0	0.0622	8.80
	377	389.0	0.0840	
	415	411.5	0.2396	
$SeOCl_3^-$ [c]	116	57.3	0.0280	
	135	102.9	0.0353	
	168	108.6	0.0725	
	229	199.1		
	243	205.8		
	291	231.9		
	326	288.5		
	336	315.9		
	953	980.6		
$SeOCl_2$	161	138.9	0.0532	9.77
	255	229.1	0.0763	
	279	258.2	0.1223	
	347	341.8		
	388	370.2		
	995	1000.9		
$SeBr_3^-$		33.1	0.0111	
		68.0	0.0159	
		97.9	0.0368	
		147.4		
		172.1		
		255.5		
$SeBr_2$		99.7	0.0262	11.38
		286.5	0.0317	
		291.6	0.1514	
$TeCl_3^-$		67.4	0.0261	
		109.5	0.0359	
		121.7	0.0954	
		214.7		
		234.7		
		332.4		
$TeCl_2$	125	125.8	0.0515	10.33
		358.4	0.0753	
	377	376.4	0.1632	

[a] Experimental frequencies are from ref 35 unless otherwise noted. [b] Present work, calculated at the B3LYP/aug-cc-pVTZ level. [c] Reference 22.

charge distributions (natural population analysis)[39] in these systems. No symmetry restrictions were used in the optimizations, and reasonable alternative geometries were checked to ensure that global minima were found.

Computational methods for some of the heavy atoms studied here are not fully developed, and limitations on computational resources make some other calculations impractical. G2 and B3LYP calculations were performed where possible, based on their accuracy in anionic test cases.[40] G2 and B3LYP/ 6-311+G-(d) calculations on the Te-containing compounds were not done because the necessary basis sets are unavailable for Te. G2 calculations for $SeBr_3^-$ were not done because of the size of the calculations. In other calculations, the aug-cc-pVTZ basis set[41] was used for molecules that contained Se, and the SDB-aug-cc-pVTZ basis set[42] (which uses the SDB core for elements heavier than Ar) was used for Te-containing molecules. For brevity all of these calculations are elsewhere in the text described as aug-cc-pVTZ. Calculations from both basis sets on the Se/Cl/O compounds gave essentially the same bond energies and atomic charges.

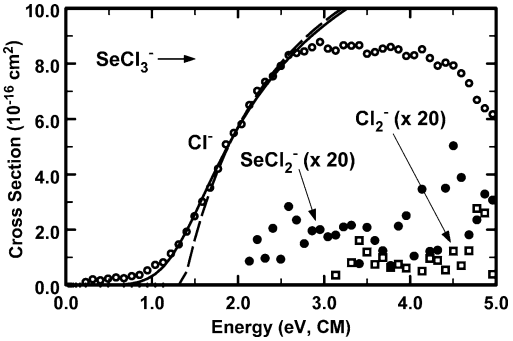

Figure 1. Cross section for collision-induced dissociation of $SeCl_3^-$ as a function of energy in the center-of-mass frame. Solid and dashed lines represent convoluted and unconvoluted fits to the data, as discussed in the text.

Results and Discussion

CID of all four anions gives loss of a halide anion as the predominant product. Loss of a halogen atom or a dihalogen molecule/anion are also observed. The dissociation products are delineated in reactions 3−14. For all reactants, the two minor products each account for 1−3% of the total reaction cross section at higher energies.

$$SeCl_3^- \rightarrow SeCl_2 + Cl^- \quad (3)$$

$$\rightarrow SeCl_2^- + Cl \quad (4)$$

$$\rightarrow SeCl + Cl_2^- \quad (5)$$

$$SeOCl_3^- \rightarrow SeOCl_2 + Cl^- \quad (6)$$

$$\rightarrow SeOCl_2^- + Cl \quad (7)$$

$$\rightarrow SeOCl^- + Cl_2 \quad (8)$$

$$SeBr_3^- \rightarrow SeBr_2 + Br^- \quad (9)$$

$$\rightarrow SeBr_2^- + Br \quad (10)$$

$$\rightarrow SeBr + Br_2^- \quad (11)$$

$$TeCl_3^- \rightarrow TeCl_2 + Cl^- \quad (12)$$

$$\rightarrow TeCl_2^- + Cl \quad (13)$$

$$\rightarrow TeCl + Cl_2^- \quad (14)$$

The reaction cross sections are shown in Figures 1−4; some of the minor products are not shown because the product signal was insufficient to collect useful data. The eq 2 fitting parameters for all four systems are given in Table 2, and the fits are also shown in Figures 1−4. The cross sections for minor products are negligible in the threshold region and are not included in the fit. Because the effects of reactant and product internal energy are included in the fitting procedure, the dissociation thresholds correspond to bond energies at 0 K. The final uncertainties in the bond energies are derived from the standard deviation of the thresholds determined for individual data sets, the uncertainty in the reactant internal energy, the effects of kinetic shifts, and the uncertainty in the energy scale (±0.15 eV lab). These results are given in Table 3.

The 0 K bond energies can be converted into 298 K bond enthalpies by use of the heat capacities of the reactants and

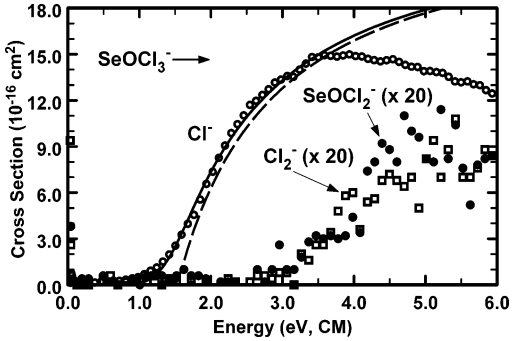

Figure 2. Cross section for collision-induced dissociation of $SeOCl_3^-$ as a function of energy in the center-of-mass frame. Solid and dashed lines represent convoluted and unconvoluted fits to the data, as discussed in the text.

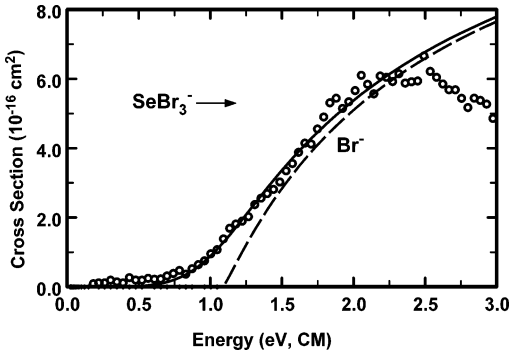

Figure 3. Cross section for collision-induced dissociation of $SeBr_3^-$ as a function of energy in the center-of-mass frame. Solid and dashed lines represent convoluted and unconvoluted fits to the data, as discussed in the text.

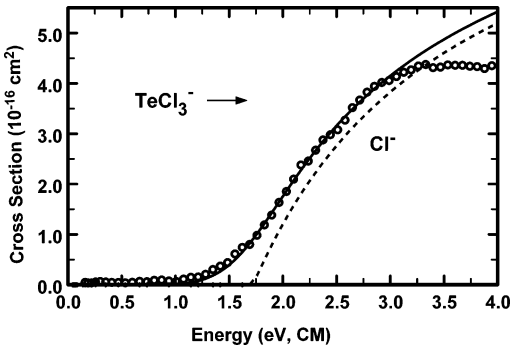

Figure 4. Cross section for collision-induced dissociation of $TeCl_3^-$ as a function of energy in the center-of-mass frame. Solid and dashed lines represent convoluted and unconvoluted fits to the data, as discussed in the text.

TABLE 2: Fitting Parameters for CID Data[a]

compd	E_T (eV)	n
$SeCl_3^-$	1.378 ± 0.089	0.95 ± 0.10
$SeOCl_3^-$	1.559 ± 0.106	1.00 ± 0.08
$SeBr_3^-$	1.136 ± 0.046	0.97 ± 0.12
$TeCl_3^-$	1.763 ± 0.044	0.97 ± 0.08

[a] See text for discussion of fitting parameters.

products, determined from the vibrational frequencies in Table 1. Very similar heat capacities for reactants and products mean that the 298 K bond enthalpies are essentially the same as the 0 K enthalpies.

Molecular Geometries. Calculations on the molecules relevant to this study were done by use of several techniques and basis sets; the optimized geometries are not very dependent on the basis set chosen. The geometries calculated by the B3LYP/aug-cc-pVTZ method are given in Table 4, and representative examples are shown in Figure 5. The anions studied have five bonds or lone pairs around the central chalcogen atom, so the ChX_3^- ions (X = Cl or Br) have T-shaped geometries and the $ChOX_3^-$ ions are disphenoidal (seesaw shaped). The neutral dissociation products are bent (ChX_2) or pyramidal ($ChOX_2$).

TABLE 3: Bond Dissociation Enthalpies[a]

system	exp	exp 298 K	B3LYP/ aug-cc-pVTZ	B3LYP/ 6-311+G(d)	G2 (298 K)
SCl_3^-	85 ± 8	85 ± 8	108	118	99
$SOCl_3^-$	85 ± 8	85 ± 8	121	135	103
$SeCl_3^-$	133 ± 9	133 ± 9	140.0	147.7	133
$SeOCl_3^-$	150 ± 10	150 ± 10	152.3	159.8	143
$SeBr_3^-$	110 ± 6	109 ± 6	131.4	130.7	
$TeCl_3^-$	170 ± 7	170 ± 7	167.0		
$TeOCl_3^-$			182.0		

[a] Values are in kilojoules per mole at 0 K unless otherwise stated.

Experimental geometries for SCl_2,[43] $SOCl_2$,[44] $SeCl_2$,[32] $SeOCl_2$,[45,46] and $TeCl_2$[47] are available; these are compared to the calculated results in Table 4. The calculated bond lengths are longer than the experimental values by 0.01−0.05 Å; this slight but consistent overestimate is typical for this type of calculation.[28,48] The calculated angles agree well with experiment except that the calculated Cl−Se−Cl angle in $SeOCl_2$ is larger by 7°. For the discussion below, the calculated results will be used for consistency.

Addition of an oxygen atom to $ChCl_2$ does not change the number of ligands plus lone pairs around the central atom, so it does not greatly alter the geometry, lengthening the Ch−Cl bonds by 0.03 Å (Ch = Te) to 0.08 Å (Ch = S). Addition of an oxygen atom to $ChCl_3^-$ has similar effects, increasing Ch−Cl bond lengths by 0.01−0.11 Å. Again, the S−Cl bond lengths change the most while the Te−Cl bond lengths increase the least.

Addition of a chloride to $ChCl_2$ or $ChOCl_2$ does change the number of ligands and the electron count on the central atoms; the calculated geometries change substantially. The equatorial bond lengths in ChX_3^- and $ChOX_3^-$ are 0.04−0.07 Å longer than in ChX_2 and $ChOX_2$. A much greater difference is seen in the axial bonds, which are longer by 0.23−0.34 Å (again, the bond lengths increase in the order Te < Se < S).

A simple bonding descriptor, initially applied to van der Waals complexes, clarifies these bond length changes. Reed et al.[49] defined the *covalency ratio* χ:

$$\chi = (R_{vdW} - d_{AB})/(R_{vdW} - R_{cov}) \qquad (15)$$

where d_{AB} is the interatomic distance and R_{vdW} and R_{cov} are respectively the sums of the two van der Waals radii and covalent radii for the bonding atoms.[50] A purely covalent bond has $\chi = 1$, and a purely van der Waals interaction has $\chi = 0$. This model normalizes differences in bond distances in a straightforward way. It should be noted that the model does not distinguish between covalent and ionic bonding. Also, the correlation between bond length and bond strength is not necessarily linear.

The computed bond lengths given in Table 4 give χ values ranging from 0.93 to 1.00 for Ch−X bonds in the neutral species. This agrees with expectations for these molecules with nominal single bonds. The equatorial Ch−X bonds in the anions have slightly lower values, $\chi = 0.88-0.97$, while for the axial bonds $\chi = 0.71-0.84$. In each category the S-containing chlorides have the lower χ values and the Te-containing

TABLE 4: Experimental and Calculated Structures[a]

compd	method	r(Ch−O)	r(Ch−X)	∠(X−Ch−X)	∠(X−Ch−O)	χ^b	r(X−X)
SCl_2	exp[c]		2.014	102.7			
	calc		2.050	103.9		0.97	3.228
$SOCl_2$	exp[d]	1.428	2.074	97.0	108.0		
	calc	1.446	2.126	98.3	108.0	0.93	3.216
$SeCl_2$	exp[e]		2.157	99.6			
	calc		2.181	101.9		0.99	3.388
$SeOCl_2$	exp[f]	1.612	2.204	96.8	105.8		
	exp[g]	1.592	2.183	96.4	104.0		
	calc	1.602	2.240	103.4	106.0	0.95	3.516
$SeBr_2$	calc		2.339	103.4		0.98	3.672
$TeCl_2$	exp[h]		2.329	97.0			
	calc		2.340	99.8		1.00	3.579
$TeOCl_2$	calc	1.772	2.368	96.6	104.1	0.98	3.535
SCl_3^-	calc		2.392 (ax)	166.8 (ax)		0.76 (ax)	3.343
			2.086 (eq)	96.6 (eq)		0.95 (eq)	
$SOCl_3^-$	calc	1.450	2.466 (ax)	153.1 (ax)	100.0 (ax)	0.71 (ax)	3.463
			2.194 (eq)	95.8 (eq)	106.5 (eq)	0.88 (eq)	
$SeCl_3^-$	calc		2.476(ax)	167.3 (ax)		0.79 (ax)	3.511
			2.230(eq)	96.6 (eq)		0.95 (eq)	
$SeOCl_3^-$	calc	1.605	2.520 (ax)	155.4 (ax)	98.9 (ax)	0.77 (ax)	3.594
			2.314 (eq)	95.9 (eq)	104.6 (eq)	0.90 (eq)	
$SeBr_3^-$	calc		2.640 (ax)	157.7 (ax)		0.78 (ax)	3.895
			2.399 (eq)	101.2 (eq)		0.94 (eq)	
$TeCl_3^-$	calc		2.594 (ax)	174.4 (ax)		0.84 (ax)	3.610
			2.386 (eq)	92.8 (eq)		0.97 (eq)	
$TeOCl_3^-$	calc	1.779	2.599 (ax)	164.7 (ax)	96.6 (ax)	0.83 (ax)	3.627
			2.431 (eq)	92.2 (eq)	103.2 (eq)	0.94 (eq)	

[a] Bond lengths are given in angstroms; angles are given in degrees. Calculated values are from B3LYP/aug-cc-pVTZ. "ax" and "eq" refer to axial and equatorial halogens, respectively. [b] Covalency ratio for Ch−X bond (see text for discussion). [c] Reference 43. [d] Reference 44. [e] Reference 32. [f] Reference 45. [g] Reference 46. [h] Reference 47.

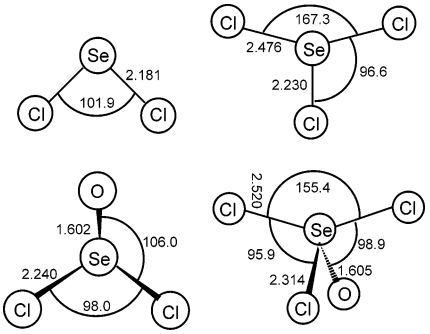

Figure 5. B3LYP/aug-cc-pVTZ-optimized geometries of representative molecules. All distances are in angstroms, and all angles are in degrees.

chlorides have the higher χ value. The selenium bromides have intermediate χ values.

Ligand Close Packing. These covalency ratios are consistent with the ligand close packing (LCP) model, which emphasizes the effects of ligand−ligand repulsion in systems where the ligands are sufficiently crowded.[51] The van der Waals radii of Cl and Br are 1.8 and 1.9 Å,[50] so repulsion is expected between any pair of chlorine atoms closer than 3.6 Å or bromine atoms closer than 3.8 Å. The closest ligand−ligand distances in the chlorides studied are 3.22−3.63 Å, with the ordering S < Se < Te for any set of corresponding systems. In the anions, there is an anticorrelation between the $Cl_{ax}-Cl_{eq}$ distances and the covalency ratios, indicating a balance between the energy cost of ligand−ligand (and ligand−lone pair) repulsion and stretched covalent bonds.[51] The fact that the axial bonds are significantly stretched while the equatorial bonds are only slightly stretched is typical of systems with five electron clouds around the central atom.[51]

The deviation of the anion $X_{ax}-Ch-X_{ax}$ bond angles from 180° is greatest for Ch = S and least for Ch = Te. This can also be explained by ligand−ligand repulsion. The bending of the axial chlorides away from the equatorial chloride implies that the equatorial chloride, which has some buildup of negative charge, is sterically more demanding than chalcogen lone pairs. However, the overestimate of the Cl−Se−Cl bond angle in $SeOCl_2$ suggests that the computational method used overestimates ligand−ligand repulsion in comparison to ligand−lone pair repulsion.

The fact that some chlorine−chlorine distances are about 10% shorter than the van der Waals contact distance should not be overemphasized. Different values of the van der Waals radii have been proposed,[52] and corrections for the atomic charge and the angular dependence of the van der Waals radii[52,53] have not been included in this work. There are many experimental examples of Cl−Cl distances below 3.6 Å,[54] indicating that the chloride ligand is relatively compressible.[51] Nevertheless, the correspondence between Cl−Cl distances, covalency ratios, and bond angles indicates that steric crowding is a significant factor in these molecules.

The Br−Br distances are 3.67 and 3.90 Å. These suggest little repulsion between the bromide ligands with Ch = Se, which is consistent with the stability of $SeBr_4$.

Molecular Orbital Approaches. The hypervalent bonding in the anions discussed in this work can be interpreted by use of the three-center four-electron (3c−4e) model,[3,9,55−58] where collinear p orbitals on the central chalcogenide atom and the two axial atoms are used to form three molecular orbitals. According to the 3c−4e model, four electrons are in two axially aligned orbitals, one bonding and the other nonbonding. On the central atom, sp^2 orbitals point toward the three equatorial positions, where there is either the equatorial halogen (with a two-center, two-electron bond to Ch), an oxygen atom, or a lone pair. Molina and Dobado[8] found some 3c−4e character in T-shaped hypervalent systems such as ChX_3^-. NBO[38] results for all anions studied in this paper indicate that the central chalcogen atom and the axial halogen atoms are involved in a

three-center, four-electron bond. This interpretation is consistent with the bond length changes described above: the equatorial bond remains largely a two-center, two-electron bond while the bonds that lengthen substantially change from 2c−2e bonding to 3c−4e bonding.[59]

This bonding description is oversimplified in that there is mixing between the orbitals involved in the 3c−4e bond and other orbitals in the molecule. Hoffmann and co-workers[9] have given an extensive description of additional orbital interactions that can have a substantial influence on the strengths of hypervalent bonds. These effects, however, should be relatively similar in the set of anions studied.

Another potentially significant interaction in these systems is negative hyperconjugation (n → σ^* delocalization),[3,60] including electron donation from lone pairs on the halogens into antibonding Ch−X orbitals. Iwaoka et al.[61] calculated that certain fluoride−organoselenium bonding interactions had a $n_F \rightarrow \sigma^*_{Se-X}$ character. Hyperconjugation involving chalcogen lone pairs as donors has also been discussed.[26,62] Hyperconjugation is consistent with the increase in the Ch−X equatorial bond lengths (Table 4). When a halide anion is added to the neutral molecules studied, the bond lengths increase more in the oxygenated species, which may be due to $n_O \rightarrow \sigma^*_{Se-X}$ donation. However, different amounts of steric crowding may cause this effect. Hyperconjugation is also likely to increase for larger, more electropositive central atoms, consistent with the observed trends in bond strengths. Thus, both the LCP model and the molecular orbital approach predict similar trends in agreement with the measured and calculated molecular properties.

Computational Bond Energies. The calculated bond energies are more dependent than the molecular geometries on the basis set chosen. Table 3 gives bond energies calculated with several methods and basis sets. The available G2 bond energies are 7−18 kJ mol^{-1} lower than the B3LYP/aug-cc-pVTZ results. Similarly, G2 bond strengths for phosphorus halide anions are 5−13 kJ mol^{-1} lower than B3LYP/aug-cc-pVTZ values.[14]

The G2 results for the selenium systems are 0−7 kJ mol^{-1} lower than experiment, while the B3LYP/aug-cc-pVTZ results are 2−7 kJ mol^{-1} higher than experiment. These differences are less than the experimental uncertainties. In contrast, the G2 and B3LYP/aug-cc-pVTZ bond energies in the sulfur analogues are 14−18 kJ mol^{-1} and 23−36 kJ mol^{-1} higher than experiment. Surprisingly, the agreement between experiment and theory is substantially better for the selenium systems than the sulfur systems.

A recent review[63] of the accuracy of various techniques for computing electron affinities found the best agreement with experiment with very resource-intensive models (average absolute error 0.06 eV for G2). Hybrid density functional methods with relatively large basis sets give somewhat larger average absolute errors (0.12 eV with B3LYP/aug-cc-pVTZ). Since calculated bond energies in anions depends on accurate values for the electron affinities of the reactant and product ions, uncertainties in the thermochemistry discussed in this work should be similar. An advantage of the bond strength calculations done for this work is that all of the species involved have closed-shell electronic structures, while radicals are involved in all electron affinity calculations.

The B3LYP/6-311+G(d) results are 10−21 kJ mol^{-1} higher than experiment for the selenium-containing systems, which is better agreement than seen previously for the sulfur-containing systems. They are generally higher than the other computational results discussed here. B3LYP/6-311+G(d) also gave results averaging 10 kJ mol^{-1} higher than B3LYP/aug-cc-pVTZ in related phosphorus-containing systems.[14]

TABLE 5: Natural Population Analysis Charges[a]

molecule	Ch	O	hal (ax)	hal	hal (eq)
SCl_3^- [b]	0.22		−0.51		−0.20
SCl_2 [b]	0.25			−0.13	
$SOCl_3^-$ [c]	1.32	−0.85	−0.58		−0.31
$SOCl_2$ [c]	1.26	−0.82		−0.22	
$SeCl_3^-$	0.40		−0.55		−0.31
$SeCl_2$	0.44			−0.22	
$SeOCl_3^-$	1.51	−0.94	−0.59		−0.39
$SeOCl_2$	1.47	−0.88		−0.29	
$SeBr_3^-$	0.19		−0.48		−0.24
$SeBr_2$	0.22			−0.11	
$TeCl_3^-$ [d]	0.59		−0.59		−0.40
$TeCl_2$ [d]	0.69			−0.35	
$TeOCl_3^-$ [d]	1.87	−1.11	−0.64		−0.48
$TeOCl_2$ [d]	1.86	−1.05		−0.40	

[a] Values calculated with the NBO program and B3LYP/aug-cc-pVTZ unless otherwise noted. [b] Reference 1. [c] Reference 2. [d] B3LYP/SDB-aug-cc-pVTZ basis set was used.

Comparison of Chalcogenides. Theory and experiment agree that the Se−Cl$^-$ bond in the systems studied here are substantially stronger than the corresponding S−Cl$^-$ bonds, while the Te−Cl$^-$ bonds are somewhat stronger still. The bond strengths in the group 15 tetrachloride anions are also much stronger for heavier central elements: PCl_4^-, $AsCl_4^-$, and $SbCl_4^-$ are bound by 90 ± 7, 115 ± 7, and 161 ± 8 kJ mol^{-1}, respectively.[64] However, the Pauling electronegativities of P, As, and Sb (2.19, 2.18, and 2.05, respectively) are very similar, as are the values for S and Se (2.58 and 2.55; the Te value is 2.10). Thus, central atom electronegativity is not well correlated with group 15 or 16 hypervalent bond strengths.

The covalent radii for S, Se, and Te are 1.02, 1.17, and 1.35 Å, respectively.[12] The radii therefore show a stronger correlation with bond strengths than do the electronegativities. A correlation is seen between hypervalent bond strengths and covalent atomic radii of the central atoms in 10-electron complexes of elements from groups 14 through 17;[11] work on this topic is continuing.

The $SeBr_2$−Br$^-$ bond is 23 kJ mol^{-1} weaker than the $SeCl_2$−Cl$^-$ bond. For comparison, D(PBr_3−Br$^-$) is 24 kJ mol^{-1} weaker than D(PCl_3−Cl$^-$). This is consistent with the idea that smaller (or more electronegative) elements are thermodynamically preferred for the terminal positions.

Charge Distributions. The natural population analysis charge distributions, given in Table 5, allow several comparisons of the molecules in this study to be made. The axial halides have charges from −0.48 to −0.64, consistent with the approximate 3c−4e molecular orbital picture where each axial atom has a charge of −0.5. The deviations, as well as the negative charge on the other chlorine atoms (−0.22 to −0.39), are explained by the electronegativities of the atoms involved. The chalcogen atoms in $ChCl_2$ and $ChCl_3^-$ have a moderately positive charge ranging from 0.22 to 0.69, and there is only slight reduction upon addition of the negatively charged chloride. The charges in $ChOCl_2$ and $ChOCl_3^-$ are much more positive, ranging from 1.26 to 1.87; addition of oxygen increases the charge on Ch by 1.01 to 1.28. The corresponding oxygen charges range from −0.82 to −1.11. This is consistent with viewing the Ch−O bond as mostly a Ch$^+$−O$^-$ interaction. Very similar trends are also calculated for related phosphorus-containing systems such as $POCl_3$ and $POCl_4^-$.[14]

Since the chlorine atoms are negatively charged, greater positive charge on the chalcogen should increase the Ch−Cl$^-$ bond strengths through electrostatic attraction, making $ChOCl_3^-$

more strongly bound than $ChCl_3^-$. This is the case for Ch = Se and Te, but the effect is small, while the experimental bond strengths in SCl_3^- and $SOCl_3^-$ are the same. It was previously noted that the oxygen atom in $SOCl_2$ does not assist in delocalizing the negative charge when Cl^- is added to the molecule.[2] This is also true for $SeOCl_2$ and $TeOCl_2$. It is possible that the relatively small electrostatic bond strength increase is canceled for Ch = S by increased ligand−ligand repulsions, which are smaller for the larger chalcogens Se and Te.

Solvation Effects. The bond enthalpy $D(SeOCl_2-Cl^-)$ is 150 kJ mol^{-1} in the gas phase at 298 K. The constants in Table 1 can be used to calculate that ΔG for bond cleavage at 298 K is 28 kJ mol^{-1} lower than the bond enthalpy, giving a free energy change for bond cleavage of 122 kJ mol^{-1}. The corresponding ΔH and ΔG values in DMSO solution at 298 K are −24 and 6 kJ mol^{-1}, respectively.[21] Thus, solvation by DMSO weakens the bond in $SeOCl_3^-$ by 174 kJ mol^{-1} (ΔH) or 116 kJ mol^{-1} (ΔG). For comparison, the Cl_2-Cl^- bond enthalpy is lower by 97 kJ mol^{-1} in aqueous solution than in the gas phase.[65] The Cl_3^- value (and those for Br_3^- and I_3^-) are consistent with the Born model, eq 16, which states that the free energy of solvation of an ion is inversely proportional to the radius of the ion r_i.[66] Other factors in the equation include the charge on the ion (Ze), the relative permittivity of the solvent (ϵ_T, 46.8 for DMSO at 298 K),[67] and the permittivity of vacuum (ϵ_0).

$$\Delta G_{solv} = -Z^2 e^2 N_A (1 - \epsilon_T^{-1})(8\pi\epsilon_0 r_i)^{-1} \qquad (16)$$

The radius of Cl^- has been determined to be 1.80 Å.[68] The molecular volume of $SeOCl_2$, 113 Å^3, can be derived from the density of 2.44 g cm^{-3}.[69] It can then be approximated that $SeOCl_2$ and $SeOCl_3^-$ are effectively spherical, such that $V = 4\pi r^3/3$ and that the volume of $SeOCl_3^-$ equals the sum of the volumes for $SeOCl_2$ and Cl^- (24.4 Å^3). This gives a calculated radius for $SeOCl_3^-$ of 3.2 Å and a value of 165 kJ mol^{-1} for the ΔG_{sol} difference of the two anions. The main reason for the difference between the solvation effects for $SeOCl_3^-$ and Cl_3^- is presumably that Cl_3^-, with a radius of 2.55 Å,[68] is smaller than $SeOCl_3^-$.

The free energy of solvation for gaseous $SeOCl_2$ in DMSO is not known. $SeOCl_2$ is not very soluble in many organic solvents, but it is at least soluble up to 5.1 mM in DMSO.[21] This gives an upper limit for $\Delta G_{sol}(SeOCl_2$, liquid) of 13 kJ mol^{-1}. ΔG_{vap} ($SeOCl_2$, liquid) is 18 kJ mol^{-1} at 298 K.[70] Thus, ΔG for $SeOCl_{2(g)}$ dissolving in DMSO is ≤ -5 kJ mol^{-1}, where the limit is probably close to the actual value. Combining the factors above gives an estimate of the difference between the gas- and solution-phase ΔG for breaking the $SeOCl_2-Cl^-$ bond of ca. 170 kJ mol^{-1}. Given these approximations, agreement with the experimental value of 116 kJ mol^{-1} is reasonable. This indicates that the main reason for the difference in the gas-phase and solution bond energies is indeed the differential solvation of ions of different sizes.

Potential Energy Surfaces. The potential energy surfaces for the reactions of chloride with $SeCl_2$ or $SeOCl_2$ are very simple. Fixing the Se−Cl distance for the incoming nucleophile to a variety of separations and optimizing the rest of the structure of $SeCl_3^-$ and $SeOCl_3^-$ indicated no transition states or any other intermediates. The reactants come together without a barrier to form the hypercoordinate species, $SeCl_3^-$ and $SeOCl_3^-$. This same shape was observed for the potential energy surfaces for the reaction of chloride with SCl_2 or $SOCl_2$.[1,2] In all of these examples, a stable hypercoordinate sulfur or selenium anion can be created when suitably substituted with electron-withdrawing groups that stabilize the anionic charge. This is consistent with an addition−elimination nucleophilic substitution mechanism for attack at the chalcogens.

A similar map of the potential energy surface for the tellurium compounds was not carried out, but it is reasonable to expect a similar lack of barriers between the stable chloride adducts and the dissociated products. A metastable structure with two chlorides in equatorial positions and only one in an axial position was located, however. This structure is less stable than the T-shaped structure by 202 kJ mol^{-1} at the B3LYP/aug-cc-pVTZ level, so it is not likely to be experimentally accessible. Analogues for the lighter chalcogens are unlikely to be metastable because the bonding is generally weaker in these systems.

Acknowledgment. This material is based upon work supported by the National Science Foundation under Grant 9985883 (NIU). S.M.B. and J.K.F. thank the Robert A. Welch Foundation (W-1442) and the Petroleum Research Foundation, administered by the American Chemical Society, for support of this research. We thank Peter Armentrout, Mary Rodgers, and Kent Ervin for use of the CRUNCH software for data analysis and Cathy Check for assistance with some of the calculations.

References and Notes

(1) Gailbreath, B. D.; Pommerening, C. A.; Bachrach, S. M.; Sunderlin, L. S. *J. Phys. Chem. A* **2000**, *104*, 2958−2961.
(2) Bachrach, S. M.; Hayes, J. M.; Check, C. E.; Sunderlin, L. S. *J. Phys. Chem. A* **2001**, *105*, 9595−9597.
(3) Reed, A. E.; Schleyer, P. v. R. *J. Am. Chem. Soc.* **1990**, *112*, 1434.
(4) Norman, N. C. *Periodicity and the P-block Elements*; Oxford University Press: Oxford, U.K., 1994.
(5) Magnusson, E. *J. Am. Chem. Soc.* **1990**, *112*, 7940.
(6) Noury, S.; Silvi, B.; Gillespie, R. J. *Inorg. Chem.* **2002**, *41*, 2164−2172.
(7) Gillespie, R. J.; Silvi, B. *Coord. Chem. Rev.* **2002**, *233−234*, 53−62.
(8) Molina, J. M.; Dobado, J. A. *Theor. Chem. Acc.* **2001**, *105*, 328−337.
(9) Landrum, G. A.; Goldberg, N.; Hoffmann, R. *J. Chem. Soc., Dalton Trans.* **1997**, 3605−3613.
(10) Kaupp, M.; van Wüllen, Ch.; Franke, R.; Schmitz, F.; Kutzelnigg, W. *J. Am. Chem. Soc.* **1996**, *118*, 11939−11950.
(11) Check, C. E.; Lobring, K. C.; Hao, C.; Wright, B.; Banweg, N.; White, E.; Bailey, J.; Sunderlin, L. S. Manuscript in preparation.
(12) Huheey, J. E.; Keiter, E. A.; Keiter, R. L. *Inorganic Chemistry*, 4th ed.; Harper Collins: New York, 1993.
(13) (a) Larson, J. W.; McMahon, T. B. *J. Am. Chem. Soc.* **1983**, *105*, 2499. (b) Larsen, J. W.; McMahon, T. B. *J. Am. Chem. Soc.* **1985**, *107*, 766. (c) Larson, J. W.; McMahon, T. B. *Inorg. Chem.* **1987**, *36*, 4018−4023.
(14) Check, C. E.; Lobring, K. C.; Keating, P. R.; Gilbert, T. M.; Sunderlin, L. S. *J. Phys. Chem. A* **2003**, *107*, 8961−8967.
(15) Wiberg, N. *Holleman-Wiberg Inorganic Chemistry*, 1st English Ed.; Academic Press: San Diego, CA, 2001.
(16) Bachrach, S. M.; Gailbreath, B. D. *J. Org. Chem.* **2001**, *66*, 2005−2010.
(17) (a) Bachrach, S. M.; Mulhearn, D. C. *J. Phys. Chem.* **1996**, *100*, 3535−3540. (b) Bachrach, S. M.; Hayes, J. M.; Dao, T.; Mynar, J. L. *Theor. Chem. Acc.* **2002**, *107*, 266−271.
(18) Mulhearn, D. C.; Bachrach, S. M. *J. Am. Chem. Soc.* **1996**, *118*, 9415−9421.
(19) Bachrach, S. M.; Woody, J. T.; Mulhearn, D. C. *J. Org. Chem.* **2002**, *67*, 8983−8990.
(20) Bachrach, S. M.; Demoin, D.; Luk, M.; Miller, J. V. Manuscript in preparation.
(21) Wasif, S.; Salama, S. B. *J. Chem. Soc., Dalton Trans.* **1975**, 2239−2241.
(22) (a) LaHaie, P.; Milne, J. *Inorg. Chem.* **1979**, *18*, 632−637. (b) Milne, J.; LaHaie, P. *Inorg. Chem.* **1983**, *22*, 2425−2428.
(23) Paetzold, V. R.; Aurich, K. *Z. Anorg. Allg. Chem.* **1966**, *348*, 94−106.
(24) Furukawa, N.; Sato, S. Structure and Reactivity of Hypervalent Chalcogen Compounds: Selenurane (Selane) and Tellurane (Tellane). In *Chemistry of Hypervalent Compounds*; Wiley: New York, 1999.
(25) Dobado, J. A.; Martínez-García, H.; Molina, J. M.; Sundberg, M. R. *J. Am. Chem. Soc.* **1999**, *121*, 3156−3164.

(26) Fowler, J. E.; Schaefer, H. F., III. *J. Am. Chem. Soc.* **1994**, *116*, 9596−9601.
(27) Minyaev, R. M.; Minkin, V. I. *Can. J. Chem.* **1998**, *76*, 776−788.
(28) Li, Q.; Xu, W.; Xie, Y.; Schaefer, H. F., III. *J. Phys. Chem. A* **1999**, *103*, 7496−7505.
(29) Muntean, F.; Armentrout, P. B. *J. Chem. Phys.* **2001**, *115*, 1213−1228 and references therein.
(30) Armentrout, P. B. *J. Am. Soc. Mass Spectrom.* **2002**, *13*, 419−434.
(31) Do, K.; Klein, T. P.; Pommerening, C. A.; Sunderlin, L. S. *J. Am. Soc. Mass Spectrom.* **1997**, *8*, 688−696.
(32) Fernholt, L.; Haaland, A.; Seip, R.; Kniep, R.; Korte, L. *Z. Naturforsch. B* **1983**, *38B*, 1072−1073.
(33) (a) Ervin, K. M.; Armentrout, P. B. *J. Chem. Phys.* **1985**, *83*, 166−189. (b) Rodgers, M. T.; Ervin, K. M.; Armentrout, P. B. *J. Chem. Phys.* **1997**, *106*, 4499.
(34) Robertson, E. G.; McNaughton, D. *J. Phys. Chem. A* **2003**, *107*, 642−650.
(35) Nakamoto, K. *Infrared and Raman Spectra of Inorganic and Coordination Compounds Part A*: *Theory and Applications in Inorganic Chemistry*, 5th ed.; John Wiley & Sons: New York, 1997.
(36) (a) Loh, S. K.; Hales, D. A.; Lian, L.; Armentrout, P. B. *J. Chem. Phys.* **1989**, *90*, 5466. (b) Schultz, R. H.; Crellin, K. C.; Armentrout, P. B. *J. Am. Chem. Soc.* **1991**, *113*, 8590.
(37) Frisch, M. J.; Trucks, G. W.; Schlegel, H. B.; Scuseria, G. E.; Robb, M. A.; Cheeseman, J. R.; Zakrzewski, V. G.; Montgomery, J. A., Jr.; Stratmann, R. E.; Burant, J. C.; Dapprich, S.; Millam, J. M.; Daniels, A. D.; Kudin, K. N.; Strain, M. C.; Farkas, O.; Tomasi, J.; Barone, V.; Cossi, M.; Cammi, R.; Mennucci, B.; Pomelli, C.; Adamo, C.; Clifford, S.; Ochterski, J.; Petersson, G. A.; Ayala, P. Y.; Cui, Q.; Morokuma, K.; Malick, A D.; Rabuck, K. D.; Raghavachari, K.; Foresman, J. B.; Cioslowski, J.; Ortiz, J. V.; Baboul, A. G.; Stefanov, B. B.; Liu, G.; Liashenko, A.; Piskorz, P.; Komaromi, I.; Gomperts, R.; Martin, R. L.; Fox, D. J.; Keith, T.; Al-Laham, M. A.; Peng, C. Y.; Nanayakkara, A.; Challacombe, M.; Gill, P. M. W.; Johnson, B.; Chen, W.; Wong, M. W.; Andres, J. L.; Gonzalez, C.; Head-Gordon, M.; Replogle, E. S.; Pople, J. A. *Gaussian 98*, revision A.9; Gaussian, Inc.: Pittsburgh, PA, 1998.
(38) Glendening, E. D.; Badenhoop, J. K.; Reed, A. E.; Carpenter, J. E.; Bohmann, J. A.; Morales, C. M.; Weinhold, F. *NBO 5.0*; Theoretical Chemistry Institute, University of Wisconsin, Madison WI, 2001. http://www.chem.wisc.edu/~nbo5.
(39) (a) Reed, A. E.; Weinhold, F. *J. Chem. Phys.* **1983**, *78*, 4066−4073. (b) Reed, A. E.; Weinstock, R. B.; Weinhold, F. *J. Chem. Phys.* **1985**, *83*, 735−746.
(40) Rienstra-Kiracofe, J. C.; Tschumper, G. S.; Schaefer, H. S., III; Nandi, S.; Ellison, G. B. *Chem. Rev.* **2002**, *102*, 231−282.
(41) (a) Dunning, T. H., Jr. *J. Chem. Phys.* **1989**, *90*, 1007−1023. (b) Kendall, R. A.; Dunning, T. H., Jr.; Harrison, R. J. *J. Chem. Phys.* **1992**, *96*, 6796−6806. (c) Woon, D. E.; Dunning, T. H., Jr. *J. Chem. Phys.* **1993**, *98*, 1358−1371. (d) Wilson, A. K.; Woon, D. E.; Peterson, K. A.; Dunning, T. H., Jr. *J. Chem. Phys.* **1999**, *110*, 7667−7676.
(42) (a) Martin, J. M. L.; Sundermann, A. *J. Chem. Phys.* **2001**, *114*, 3408−3420. (b) Bergner, A.; Dolg, M.; Kuechle, W.; Stoll, H.; Preuss, H. *Mol. Phys.* **1993**, *80*, 1431.
(43) Bizzocchi, L.; Cludi, L.; Degli Esposti, C.; Giorgi, A. *J. Mol. Spectrosc.* **2000**, *204*, 275−280.
(44) Mata, F.; Carballo, N. *J. Mol. Struct.* **1983**, *101*, 233−238.
(45) Gregory, D.; Hargittai, I.; Kolonits, M. *J. Mol. Struct.* **1976**, *31*, 261−267.
(46) Zharskii, I. M.; Zasorin, E. Z.; Spiridonov, V. P.; Novikov, G. I. *Vestnik Moskovskogo Universiteta, Ser. 2* **1977**, *18*, 166−169 (CAS abstract 87: 141630).
(47) Fernholt, L.; Haaland, A.; Volden, H. V.; Kniep, R. *J. Mol. Struct.* **1985**, *128*, 29−31.
(48) Sánchez Márquez, J.; Fernández Núñez, M. *J. Mol. Struct.* **2003**, *624*, 239−249.
(49) Reed, A. E.; Curtiss, L. A.; Weinhold, F. *Chem. Rev.* **1988**, *88*, 899−926.
(50) van der Waals radii of 1.8, 1.9, 2.1, 1.8, and 1.9 Å for S, Se, Te, Cl, and Br, respectively; covalent radii of 1.02, 1.17, 1.35, 0.99, and 1.14 Å. Data are from ref 12.
(51) Robinson, E. A.; Gillespie, R. J. *Inorg. Chem.* **2003**, *42*, 3865−3872.
(52) Badenhoop, J. K.; Weinhold, F. *J. Chem. Phys.* **1997**, *107*, 5422−5432.
(53) Batsanov, S. S. *Russ. J. Gen. Chem.* **2002**, *72*, 1153−1156.
(54) Batsanov, S. S. *J. Mol. Struct.* **1999**, *468*, 151−159.
(55) Hach, R. J.; Rundle, R. E. *J. Am. Chem. Soc.* **1951**, *73*, 4321−4324.
(56) (a) Heard, G. L.; Marsden, C. J.; Scuseria, G. E. *J. Phys. Chem.* **1992**, *96*, 4359−4366. (b) Novoa, J. J.; Mota, F.; Alvarez, S. *J. Phys. Chem.* **1988**, *92*, 6561−6566. (c) Gutsev, G. L. *Russ. J. Phys. Chem.* **1992**, *66*, 1596−1599. (d) Cahill, P. A.; Dykstra, C. E.; Martin, J. C. *J. Am. Chem. Soc.* **1985**, *107*, 7, 6359−6362.
(57) Pimentel, G. C. *J. Chem. Phys.* **1951**, *19*, 446.
(58) Kaupp, M.; van Wüllen, Ch.; Franke, R.; Schmitz, F.; Kutzelnigg, W. *J. Am. Chem. Soc.* **1996**, *118*, 11939−11950.
(59) Mingos, D. M. P. *Essential Trends in Inorganic Chemistry*; Oxford University Press: Oxford, U.K., 1998; Chapter 4.
(60) Schleyer, P. v. R.; Kos, A. J. *Tetrahedron* **1983**, *39*, 1141−1150.
(61) Iwaoka, M.; Komatsu, H.; Katsuda, T.; Tomoda, S. *J. Am. Chem. Soc.* **2002**, *124*, 1902−1908.
(62) Salzner, U.; Schleyer, P. v. R. *J. Am. Chem. Soc.* **1996**, *115*, 10231−10236.
(63) Rienstra-Kiracofe, J. C.; Tschumper, G. S.; Schaefer, H. S., III; Nandi, S.; Ellison, G. B. *Chem. Rev.* **2002**, *102*, 231−282.
(64) Walker, B. W.; Check, C. E.; Lobring, K. C.; Pommerening, C. A.; Sunderlin, L. S. *J. Am. Soc. Mass Spectrom.* **2002**, *13*, 469−476.
(65) Nizzi, K. N.; Pommerening, C. A.; Sunderlin, L. S. *J. Phys. Chem. A* **1998**, *102*, 7674−7679.
(66) Atkins, P.; de Paula, J. *Physical Chemistry*, 7th ed.; Freeman: New York, 2002; Chapter 10.
(67) Wohlfarth, C. Permittivity (Dielectric Constant) of Liquids. In *CRC Handbook of Chemistry and Physics*, 83rd ed; Lide, D. R., Ed.; CRC Press: Boca Raton, FL, 2002.
(68) Marcus, Y. *Ion Properties*; Marcel Dekker: New York, 1997.
(69) Physical Constants of Inorganic Compounds. In *CRC Handbook of Chemistry and Physics*, 83rd ed; Lide, D. R., Ed.; CRC Press: Boca Raton, FL, 2002.
(70) Yaws, C. L. *Handbook of Vapor Pressure*; Gulf Publishing: Houston, TX, 1995; Vol. 4.